

## RESEARCH ARTICLE

# ANATOMY OF THE AXIAL AND PELVIC LIMB BONES OF THE WEST AFRICAN BLACK-CROWNED CRANE (*BALEARICA PAVONINA PAVONINA*)

Ibrahim Alhaji Girgiri, Ali Musa Wolgo, Mohammed Malah Kachallah, Waziri Alhaji Kachamai, Isa Shehu Nuhu

Department of Veterinary Anatomy,  
Faculty of Veterinary Medicine,  
University of Maiduguri, Borno State,  
Nigeria

**Corresponding author:**

Dr. Ibrahim Alhaji Girgiri

**Address:** Head, Department of  
Veterinary Anatomy, Faculty of  
Veterinary Medicine, University of  
Maiduguri, Borno State, Nigeria

**Phone:** +234 7035108133

**ORCID:**0000-0002-606-9953

**Email:** ibrahimgirgiri@unimaid.edu.ng

**Original Submission:** 13 May 2023

**Revised Submission:** 9 July 2023

**Accepted:** 7 September 2023

**How to cite this article:** Girgiri IA, Wolgo AM, Kachallah MM, Kachamai WA, Nuhu IS. 2023. Anatomy of the axial and pelvic limb bones of the West African black-crowned Crane (*Balearica pavonina pavonina*). *Veterinaria*, 72(3), 290-301.

**ABSTRACT**

The study presented gross morphological features of the axial and pelvic limb bones of adult black-crowned crane. The bones were macerated using a standard technique and structural details of the processed bones were highlighted. The skull comprised of the splanchnocranium and neurocranium, separated by a large bony orbit. The mandible presented a rostral dental bone having minute foramina and a caudal supra-angular bone. The cranial segment of the vertebral axis consists of fifteen cervical and seven free thoracic vertebrae. The caudal portion of the vertebral column fused into a single bony column comprising of notarium, synsacro-lumbar, three-fused primary sacral, and fused three synsacro-caudal vertebrae, respectively. There were six free coccygeal vertebrae, the last presented the pygostyle. The pelvic girdle was formed by the osseous fusion of the ilium, ischium, and pubis. The maximum length of the femur was 10.5 cm, whereas the tibiotarsus was 24.5cm. The tarsometatarsus comprised of fused metatarsal bones II, III, IV which articulates with the distal row of tarsal bone. There were four functional digits in black-crowned crane. The first digit consists of two phalanges, the second and third digits presented three and four phalanges and the fourth digit consists of five phalanges.

**Keywords:** Gross anatomy, skull, axial, pelvic limb bones, black-crowned crane

## INTRODUCTION

The Black-crowned Crane *Balearica pavonina* inhabits the Sahel and Sudan Savanna regions of Africa (Edet et al., 2018). There are two Black-crowned Crane subspecies: the West African Crowned Crane (*Balearica pavonina pavonina*), which occupies the western part of the Sahel, from Senegal to Chad and the Sudan Crowned Crane (*Balearica pavonina ceciliae*) that lives in Eastern Africa, with its largest concentration in Sudan (Boere, 2006). Black crane birds had been classified as near-threatened (IUCN, 2006). The gross morphology of the sternum, pectoral girdle and wing bones of the Black-crowned Crane has been described recently (Girgiri et al., 2022). Earlier, Hiragi et al (2014) documented the vertebral formula in red-crowned and Hooded Crane. The present study was aimed at describing the gross morphology of skeleton of the Black crowned Crane with emphasis on the axial, pelvic girdle and pelvic limb bones.

## MATERIALS AND METHODS

The cadaver of an adult black-crowned crane bird (*Belearica pavonina pavonina*) was collected from the Department of Veterinary Pathology, University of Maiduguri following a postmortem examination and was processed for gross anatomical studies. The axial, pelvic girdle and limb bones were macerated and processed, as described previously (Girgiri et al., 2022). Morphology and structural details of the processed bones were studied, and metrical dimensions of long bones were measured in centimeters (cm). Photographs of the bones at different anatomical planes were taken using Nikon D90 digital camera.

## RESULTS

### Skeleton of head

The skull of Black-crowned Crane comprised of the splanchnocranium and neurocranium, separated by a large bony orbit. The facial part of the skull, which constituted the splanchnocranium, comprised of bones that formed movable articulation with one

another and with the neurocranium. The paired premaxillary bone formed the rostral portion of the upper beak and presented three processes. The frontal process of the premaxillary bone formed the dorsal border of the nasal aperture, and extended caudally, where it fused with the nasal and frontal bone. The maxillary process constituted the basal border of the nasal aperture, whereas the platinum formed the basal plate (Figure 1A-C). The lacrimal bone was small and formed the nasal border of the eye orbit, dorsally fusing with the frontal bone. The paired platinum bone flanked the vomer and extended rostrally, where it fused with the processes of the maxillary bone and caudally with the pterygoid and basihyoid bone. The zygomatic bone was rod-like, and extended caudally for articulation with the quadrate bone. The pterygoid bone was short and situated between the palatine, vomer, and the quadrate bones (Figure 1A). The nasal aperture presented a triangular outline, the base of which was formed by the frontal process of the intermaxillary bone (Figure 1A).

The neurocranium was formed by the fusion of occipital, sphenoid, temporal, parietal and the frontal bone, respectively (Figure 1A-B). The occipital bone was situated basally and constituted the caudal surface of the skull. This bone presented a dorsal (supraoccipital), squamous, bilateral part and basal part which surrounded the large foramen magnum (Figure B-C). A small but prominent hemispherical occipital condyle was present at the basioccipital bone close to the margin of the foremen magnum. A jugular process was present caudolaterally to the foramen magnum (Figure 1C). The sphenoid bone was situated at the base of the skull having two distinct parts. The basisphenoid was larger, elliptical with a centrally located body and a pair of temporal wings. It articulated with the basilar part of the occipital bone caudally and extended rostrally to articulate with the presphenoid. The presphenoid articulated with the temporal wing of the basisphenoid caudolaterally and was lined by the paired palatinum bones rostrally (Figure 1C). The temporal bone formed the caudoventral portion of the lateral wall of the skull. It consisted of the ear capsule and the

squamous portion. The ear capsule articulated with the parietal, lateral part of the occipital and the basisphenoid bones, respectively. The squamous temporal contributed to the formation of the lateral wall of the skull and presented the orbital process dorsal to the temporal fossa. The squamous temporal articulated dorsally with the frontal bone, ventrally with the sphenoid bone and caudally with the parietal bone (Figure 1A and C). The parietal bone contributed to the formation of the dorsal part of the caudal wall of the skull. It was situated between the frontal bone and the supraoccipital bone. The frontal bone formed the dorsum of the neurocranium. It was divided into the nasal orbital and caudal part (Figure B-C). The nasal part of the frontal bone was a very prominent feature, convex and extended slightly forward (Figure 1A-B).

### **Mandible**

The mandible constitutes the bones of the lower beak. It has a paired body that fused rostrally at the mandibular symphysis, presenting a V-shaped outline that conformed to the orientation of the upper beak. The mandible comprised of secondary bones that fused into a single column. The dental bone was prominent and encompassed the rostral end of the mandible. A supraangular bone was present at the dorsocaudal aspect of the body of the mandible. The articular bone was immediately caudal to the supraangular bone, and ventral to it was the angular bone. The angular bone presented two articular processes. The medial articular process was large with rounded ends, while the caudally directed articular process was narrow with pointed end. The rostral end of the mandible presented numerous pneumatic foramina (Figure 1D). The lateral aspect of the ramus of the mandible presented two fenestrae (rostral and caudal). The caudal fenestra was less prominent. *Fossa temporalis* subdivided by a crest was present at the same location of these fenestrae on the medial aspect of the ramus of the mandible. This fossa delineates the contributions of the individual bones that formed the mandible (Figure 1E).

### **Vertebral Column**

There were fifteen cervical vertebrae in Black-crowned Crane. The atlas was the first cervical vertebra and articulated with the skull cranially via the occipital condyles. It was atypical, ring-shaped with the body bearing a prominent depression caudally for articulation with the odontoid process of the axis. The dorsal arch was delicate forming the dorsal rim of the large vertebral foramen. The ventral arch presented a cranial deep articular facet for articulation with the occipital condyle. The caudal boundary of the dorsal arch articulated with the cranial articular processes of axis (Figure 2A). The second cervical vertebra was the axis. It presented atypical spinous process which was elongated and ridge-like. The odontoid process was a prominent feature which articulated with the axis rostrally. There exists a small lateral vertebral foramen ventrolaterally to the base of the spinous process. The cranial and caudal articular processes had articular facets (Figure 2B). The remaining cervical vertebrae presented characteristic vertebral body arch and cranial and caudal articular surfaces (Figure 2C). There were seven free thoracic vertebrae in the present study. The caudal portion of the vertebral column fused into a single bony column, the *synsacrum*. Approximately five thoracic vertebrae fused to form the *notarium*. The number of fused lumbar vertebrae that form *synsacro-lumbar* was difficult to establish in the present study. The primary sacral and *synsacrocaudal* (coccygeal) vertebrae comprised of three fused vertebrae, respectively. There were six free coccygeal vertebrae, the terminal (seventh) vertebra presented the *pygostyle* (Figure 3).

### **Bones of pelvic girdle**

The pelvis comprised of two hip bones formed by the osseous fusion of three primary bones consisting of the ilium, ischium, and pubis.

### **Ilium**

The paired ilium was elongated and presented with two parts, the long preacetabular part and a short, broad postacetabular part, which united cranially

with the synsacrum of the vertebrae. Cranially, this union was by osseous fusion and caudally with the transverse processes of these vertebrae via syndesmosis. Ilioneural canal was present where the ilium, the spinal and transverse processes of the synsacrothoracic vertebrae united (Figure 4A).

The dorsal surface of the ilium presented elongated shallow depression for muscle attachment, whereas the internal surface presented the *fossa renalis*, an excavation for the accommodation of the kidneys. These fossae presented a cranial, smaller part known as the ischiatic fossa, which contained the cranial middle portion of the kidney and the lumbosacral plexus. The larger, deeper caudal part of the renal fossa was the pudendal fossa, which accommodated the caudal portion of the kidney. The renal fossa extends caudally as an invagination between the postacetabular part of the ilium and the ischium to form the renal caudal recess. The lateral edge of the postacetabular ilium bears the dorsolateral iliac crest (Figure 4 A-B). The acetabulum was circular bony ring formed by the ilium and ischium. The floor of the acetabulum presented the large acetabular foramen. Caudoventrally to the acetabulum was a small, oval obturator foramen. The obturator process partially separates the obturator foramen from the ischiopubic fenestra. A strong bony prominence representing the antitrochanter was present caudodorsally to the acetabulum. (Figure 4A-C).

### Ischium

The paired ischium was a long bony plate situated caudally and ventrally to the ilioischiatic foramen. Its cranial part contributed to the formation of the caudoventral half of the acetabulum, while its caudal part presented a broad bony plate. The bony plate was roughly quadrate-shaped, thus presented four borders: the cranial border from the caudal half of the ischiatic foramen dorsally and obturator foramen ventrally, the lateral border united with the shaft of the pubis at the publiischiatic incisures, the medial border sloped inward presenting a U-shape outline when joined the opposite border, and the

caudal border that presented a blunt caudal process (Figure 4A-C).

### Pubis

The paired pubis was a thin, rib-like bony rod. The middle portion of the pubis fused with the ventral border of the ischium at the publiischiatic incisure, where it projected beyond the ischium and curved caudomedially. The cranial extremities of the pubis terminated at the oval obturator foramen (Figure 4A-C).

### Skeleton of pelvic limbs

The bones of the pelvic limbs comprised of the femur and patella, tibiotarsus and fibula, and the tarsometatarsus and digits.

### Femur

The femur was tubular and presented a strong cylindrical body. The distal extremity was more massive than the proximal ends. The maximum length of the femur was 10.5 centimeters (cm). The proximal extremity consists of a hemispherical head, a distinct neck and the trochanter. The head of the femur was directed medially for articulation with the acetabulum. A distinct margin marked the limit of the head (Figure 5). There exists a rough notch at the center of the head, the *fovea capitis*. The trochanter major of the femur is situated laterally, slightly higher than the head and articulates with the antitrochanter of the acetabulum. The trochanter major continues as a bony ridge on the proximal cranial surface of the shaft. The shaft is generally smooth, straight and consists of four surfaces. The medial surface is the distal continuation of the head and neck. The cranial surface presents the bony ridge, an extension of the trochanter major. At the caudal lateral margin of the surface, the trochanter major continues as a distinct line that runs almost two thirds of the shaft. Both the cranial and caudal surfaces presented irregular muscular lines. The distal extremity of the femur was large bearing on its cranial surface the trochlea of the femur. The medial and lateral trochleas were separated by a wide intercondylar sulcus. The lateral was partially divided by an intratrochlear groove. Each condyle bears a small epicondyle.

The medial condyle extended proximally as a thin ridge to form the medial supracondylar crest and continued proximally on the caudal surface as the caudal intermuscular line (Figure 5).

### **Tibiotarsus**

It was the paired tubular bone. The distal extremities of the tibia articulate with the proximal row of the tarsal bones. The tibia was comparatively longer than the femur. The maximum length of the tibia was 24.5 centimeters (cm). The proximal epiphysis presented the medial and lateral condyles for articulation with the condyles of the femur. The lateral condyle bears a facet on its lateral surface for articulation with the fibula. On the cranial surface of the proximal end of tibiotarsus, there exists a prominent sharp tibial crest. This crest extended from the proximal extremity towards the shaft. The caudal surface of the proximal end of tibiotarsus has the flexor fossa distally to the lateral condyle. The proximal and distal interosseous foramen was a small elongated foramen between the fibula and tibiotarsus. The shaft of the tibiotarsus was smooth and three-sided, proximally comprising of medial, lateral and caudal surfaces. Distally, it presented the cranial and caudal surfaces. The distal extremity of the tibiotarsus was characterized by the medial and lateral trochlea. A deep passage on the cranial surface of tibiotarsus proximal to its distal condyles was the extensor canal (Figure 6 A and B).

The fibula lied parallel to the long axis of the tibiotarsus and presented a prominent head known as the *capitulum*. A fibular articular facet for articulation with the tibiotarsus was present on the medial surface of the fibula. The body of the

fibula was a thin rod-like, attached to the proximal half of the lateral surface of the shaft of the tibia (Figure 6 A and B).

### **Tarsometatarsus**

This was a single long bone comprised of fused metatarsal bones II, III, IV that articulated with the distal row of tarsal bones. Metatarsal (I) was undeveloped and united ventromedially with tarsometatarsus via a ligament. The proximal extremities of tarsometatarsus presented the concave articular surfaces divided by a protuberance for articulation with the distal trochlea of tibiotarsus. The shaft of the tarsometatarsus consisted of the dorsal and plantar surfaces. The dorsal surface presented a distinct longitudinal groove, which was deep at the proximal end and became shallow distally. The plantar surface presented three longitudinally directed crests. These crests were the lateral, intermediate and medial crest of the hypotarsus. A groove existed between the medial and intermediate crests. The distal end of tarsometatarsus presented three articular trochleas of metatarsal bones II, III and IV. Lateral and medial intertrochlear notches were present between these trochleas (Figure 7 A and B).

### **Digits**

The Black-crowned Crane had four digits; the first digit was directed medio-plantarly and consisted of two phalanges. The second and third digits presented three and four phalanges, respectively, whereas the fourth digit consisted of five phalanges. The distal phalanx of each digit presented a claw-shaped structure, which formed the bony core of the claw (Figure 7A and B).

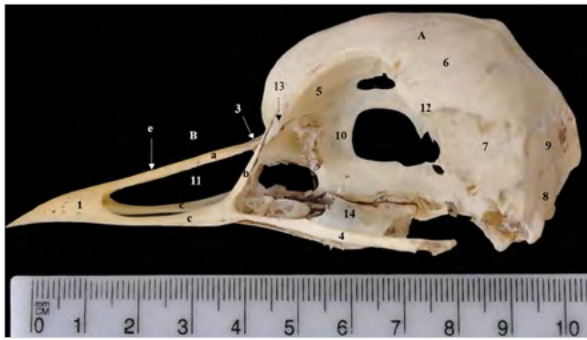


**Figure 1A** Skeleton of head of Black-crowned Crane (lateral view) showing: A. Neurocranium, B. Splanchnocranium, 1. Premaxillary bone; (e. Frontal process of premaxillary bone, c. Paired maxillary process of premaxillary bone, 3. Nasal bone; (a. Intermaxillary process, b. Maxillary process of nasal bone), 4. Zygomatic bone, 5. Ethmoidal bone, 6. Frontal bone, 7. Squamous portion of temporal bone, 8. Occipital bone, 9. Parietal bone, 10. Interorbital septum, 11. Nasal aperture, 12. Orbital process of temporal bone, 13. Lacrimal bone, 14. Platinum bone

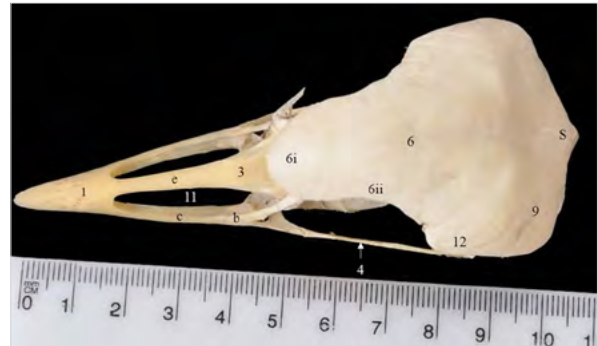


**Figure 1B** Skeleton of head of Black-crowned Crane (dorsal view) showing: 1. Premaxillary bone, e. Frontal process of premaxillary bone, c. Paired maxillary process of intermaxillary bone, 3. Nasal bone; (b. Maxillary process of nasal bone), 4. Zygomatic bone, 6. Frontal bone (6i. Nasal part, 6ii. Orbital part), 8. Occipital bone, 9. Parietal bone, S. Supraoccipital, 11. Nasal aperture



**Figure 1C** Skeleton of head of Black-crowned Crane (ventral view) showing: 1. Intermaxillary bone, a. Platinum, b. Vomer, c. Maxillary process, d. Occipital condyle, e. Frontal process of premaxillary bone, f. External acoustic pores, g. Platinum process, h. Basihyoid bone, i. Foramen magnum, j. Zygomatic bone



**Figure 1D** Mandible of Black-crowned Crane (lateral view) showing: 1. Dental bone, 3. Articular process of angular bone, 4. Supraangular bone, 5. Posterior process of angular bone



**Figure 1E** Mandible of Black-crowned Crane (dorsal view) showing: 1. Dental bone, 2. Articular bone, 3. Articular process of angular bone, 5. Posterior process of angular bone

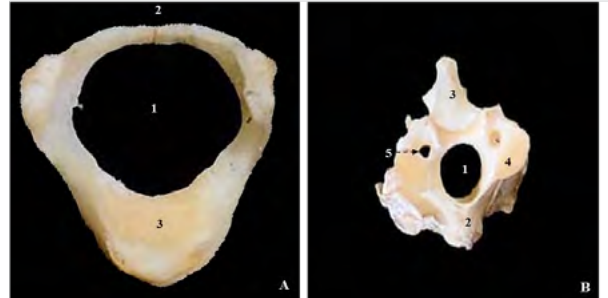


**Figure 2A-B** **A.** Atlas of Black-crowned Crane (cranial view) showing: 1. Vertebral foramen, 2. Vertebral arch, 3. Deep articular depression for odontoid process of axis. **B.** Axis of crane (cranial view) showing 1. Vertebral foramen, 2. Odontoid process, 3. Spinous process, 4. Cranial articular fovea, 5. Lateral vertebral foramen



**Figure 2C** Segment of vertebral column (cervical vertebrae  $C_3$ - $C_{12}$ ) of Black-crowned Crane (lateral view) showing: Spinous processes (thick arrow), transverse processes (thin arrow). Last two cervical vertebrae were inverted to show the transverse process. White dotted line delineates the two inverted vertebrae

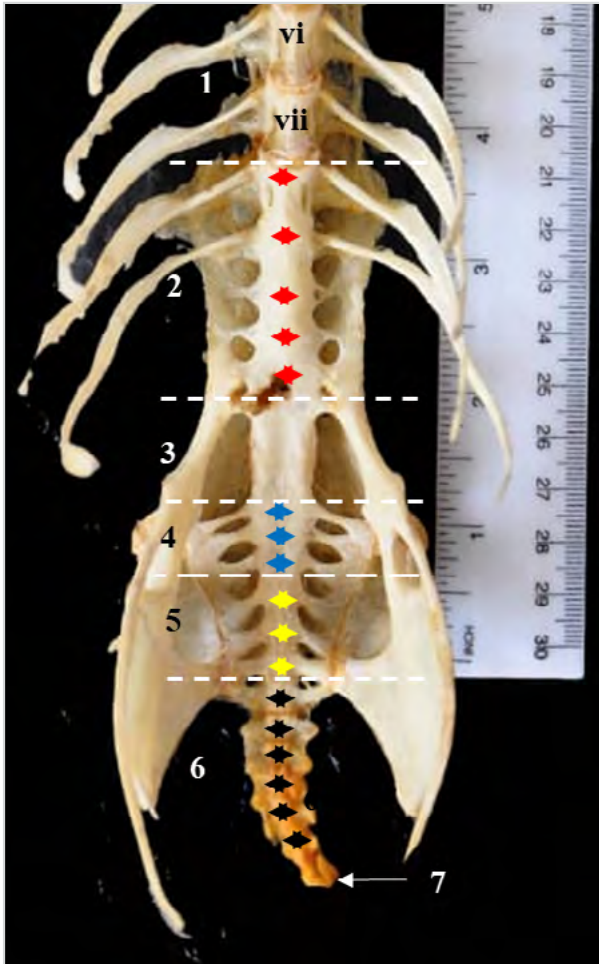


**Figure 3** Caudal part of vertebral column of Black-crowned Crane (ventral view) showing: 1. Free 6-7<sup>th</sup> thoracic vertebrae, 2. Notarium (red dots), 3. Sacrolumbar, 4. Three-fused primary sacral vertebrae (blue dots), 5. Three-fused synsacrocaudal vertebrae (yellow dots), 6. Six-fused free coccygeal vertebrae (black dots), 7. Pygostyle (white arrow). The white dotted line showed boundary between the fused vertebra forming the synsacrum

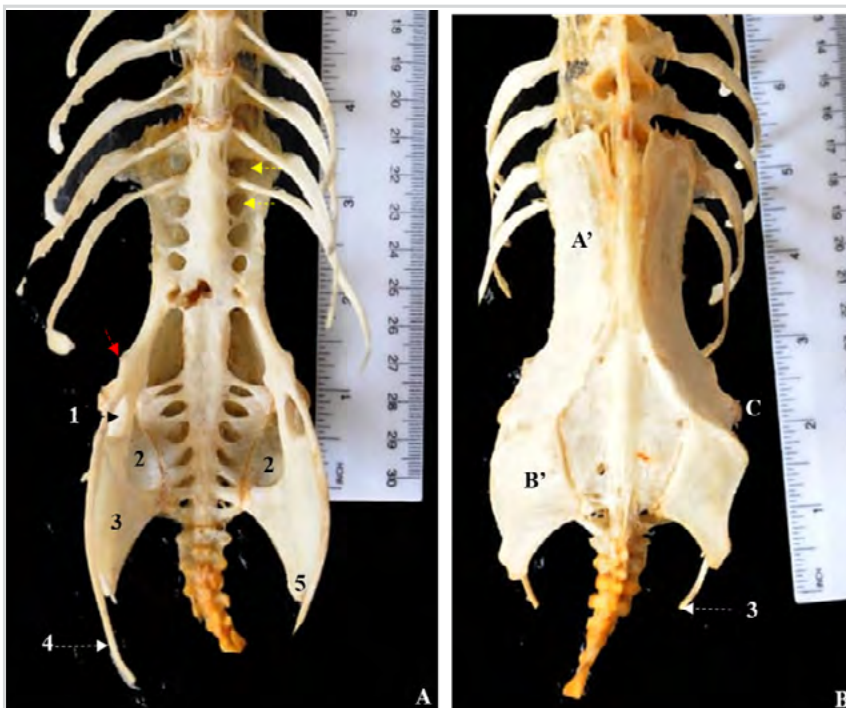


**Figure 4 A-B** A Pectoral girdle of Black-crowned Crane (ventral and dorsal view) showing: 1. Obturator foramen, 2. Renal fossa, 3. Ischium, 4. Pubis, 5. Angle of ischium; Ilioneural canal (yellow arrows), pectineal process (red arrow); **B.** A' Preactabular part of ilium, B'. Postacetabular part of ilium, C. Antitrochanter

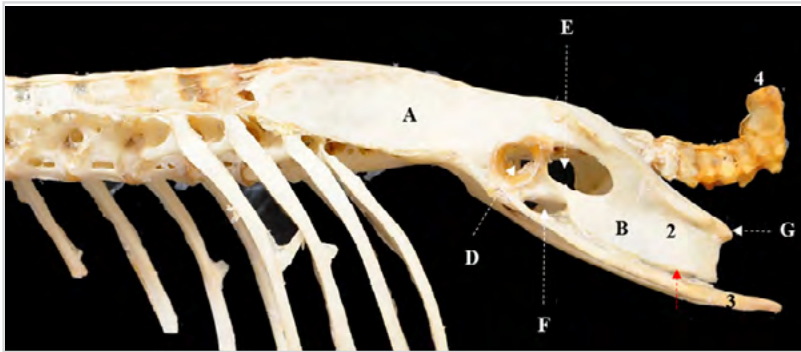


**Figure 4C** Pectoral girdle of Black-crowned Crane (lateral view) showing: A. Preacetabular part of ilium, B. Postacetabular, D. Acetabulum, E. Ischiatic foramen, F. Obturator foramen, G. Caudal process, 2. Body of ischium, 3. Pubis caudal-slit of pubis (red arrow), 4. Pygostyle

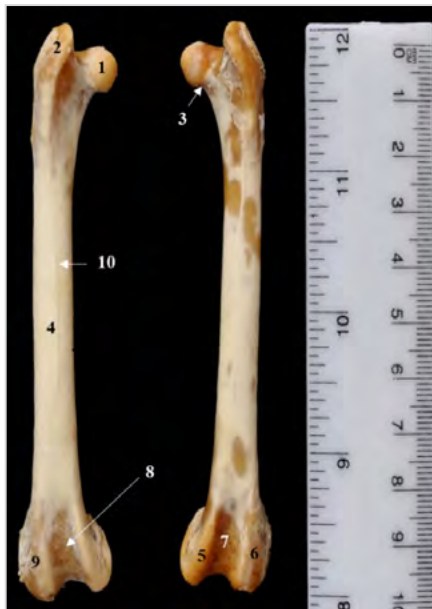


**Figure 5** Left and right femur of Black-crowned Crane (anterior view (left) and posterior view right) showing: 1. Head, 2. Trochanter major, 3. Neck, 4. Shaft, 5. Medial trochlear ridge, 6. Lateral trochlear ridge, Trochlea femoris, 8. Condylar fossa, 9. Intra-trochlear groove, 10. Muscular line

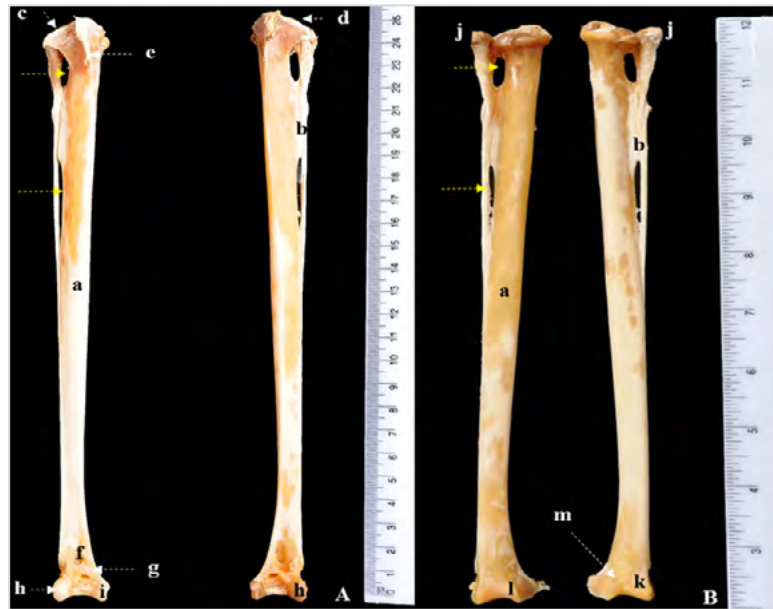


**Figure 6 A-B** Left and right tibiotarsus of Black-crowned Crane (anterior view) showing: a. Shaft of tibia, b. Shaft of fibula, c. Lateral condyle, d. Medial condyle, e. Medial crest, f. Groove, g. Bony ridge, h. Lateral trochlea, i. Medial trochlea. **B.** j. Capitulum, k. Lateral condyle, l. Medial condyle, proximal and distal interosseous space (yellow arrow)



**Figure 7** Left and right tarsometatarsus of Black-crowned Crane (A. dorsal view and planter view) showing: 1. Proximal articular facet of tarsometatarsus, articular trochlea (2-3-4) for phalanges of toes (I-IV); 5. 1<sup>st</sup> digit, 6. 2<sup>nd</sup> digit, 7. 3<sup>rd</sup> digit, 8. 4<sup>th</sup> digit, 9. Claw

## DISCUSSION AND CONCLUSION

Adult crown-birds have highly apomorphic skulls characterized by a toothless beak, enlarged round orbits, and enlarged and highly pneumatized chondrocranium (Smith-Paredes and Bhullar, 2019). The neurocranium of the Black-crowned Crane was formed by the fusion of 5-6 bones, as observed in cattle egret (Rezk, 2015) and ostrich (Moselhy et al., 2018). Olivia and Christian (2020) stated that the skulls of adult crown-birds were characterized by a high degree of integration due to bone fusion resulting in reduction of the number of bones. Some features of the bones were compared to other species owing to scarcity of literature on basic skull typology in crane bird species. The conspicuous protrusion of the nasal portion of the frontal bone is a striking feature in Black-crowned Crane. It provides for attachment of the modified plumage rostrally to the crown feathers on the head. In guinea fowl, a median ridge composed of spongy bones is present (Nickel et al., 1977). The nasal bone in Black-crowned Crane as in many birds, makes a flexible cartilaginous connection with the frontal bone, which permits the movement of the upper jaw (Dyce et al., 2010).

Hiragi et al. (2014) reported that Red-crowned and Hooded Crane had 17 cervical vertebrae with

exceptional cases having 18, fewer than 15 cervical vertebrae we recorded in Black-crowned Crane. There were 7 free thoracic vertebrae in Black-crowned Crane, whereas Red-crowned Cranes had 9-10 or 11 thoracic vertebrae, and Hooded Cranes had 9-10 (Hiragi et al., 2014). The specific number of vertebrae contributing to the formation of the synsacrum was given as 15-16 in Red-crowned Cranes and 14-16 in Hooded cranes (Hiragi et al., 2014). In the present study, the total number of vertebrae forming the synsacrum was 17, excluding the sacrolumbar where gross delineation of the fused vertebral bones was difficult to establish. The synsacrum and the notarium provide rigid support to the dorsal part of the trunk, extending laterally and caudally by the fusion of the synsacrum with the long hip bones (Dyce et al., 2010).

The pelvis of different birds presented marked morphological variations, which indicates differences in specialized locomotor function. In the present study, the preacetabular portion of the ilium is longer than the postacetabular part, as described in domestic fowl (Nickel et al., 1977; Sreeranjini et al., 2011), Crested Serpent-Eagle and Brown Wood Owl (Choudhary et al., 2020). The puboischiatic incisure presented the oval obturator foramen, caudoventral to the acetabulum

in Black-crowned Crane. The pubis of Crested Serpent-Eagle was completely fused with the ischium (Choudhary et al., 2020), whereas in emu, the pubis was separated from ischium by a large fissure except its cranial portion, which present an incomplete oval to crescent-shaped obturator foramen communicating with the fissure (Kumar and Singh, 2014). The pubis in Black-crowned Crane did not contribute to the formation of the acetabulum, as seen in domestic fowl and duck (Nickel et al., 1977). In emu, all the three primary bones of the pelvic are involved (Kumar and Singh, 2014).

The trochanter major was elevated above the head in Black-crowned Crane similar to findings in Indian Horned- Owl, flamingo and crow (Sridevi et al., 2020), whereas in emu, the trochanter major was flat and did not project above the level of the head (Kumar and Singh, 2014). A pneumatic foramen was present on the anterior surface below the trochanter major in Crested Serpent-Eagle (Choudhary et al., 2020), and in crow, small numerous pneumatic foramina (Sridevi et al., 2020). The *fovea capitis* was absent in emu (Kumar and Singh, 2014). It was eccentric in our findings, situated posteriorly-medially on the circumference of the head. The shaft is smooth and bears muscular lines on the anterior and posterior surfaces. Most of the observable features of the distal extremity of the Black-crowned Crane were similar to findings in domestic bird. A distinct groove of the caudal surface of the lateral trochlea was also reported in serpent-eagle (Choudhary et al., 2020).

In most avian species, the tibia fuses with tarsal elements, which forms a tibiotarsus that is much longer than the femur and carries the shaft of the feebly developed fibula on its lateral aspect (Dyce et al., 2010). The ratio of length tibiotarsus to femur was 1:2, as reported in emu by Kumar and Singh (2014). A sharp medial bony crest at the proximal end of tibiotarsus observed in the present study, was also reported in peahen (Sreeranjini et al.,

2013), cattle egret (Rezk, 2015) and serpent-eagle (Choudhary et al., 2020). However, medial and lateral ridges rather than the crest were observed in emu (Kumar and Singh, 2014). This crest provides for attachment of extensor muscles of the knee joint (McLelland, 1990). A nutrient foramen was reported at the middle of the lateral border of the tibia in emu (Kumar and Singh, 2014), and this has not been observed in the present study. The proximal and distal interosseous spaces in our study have been reported in serpent-eagle (Choudhary et al., 2020). The length of the tarsometatarsus was relatively long in black-crowned. This enables the bird to forage on dry ground short grass typical of Sudano-Sahelian habitat. According to Nickel et al (1977), the length of the metatarsus determines to some extent the ground clearance of the bird in standing position. The deep grooves observed on the dorsal surface of the tarsometatarsus in the present study had earlier been reported in both dorsal and plantar surfaces in emu. In addition, three nutrient foramina towards proximal extremity were seen on the dorsal surface in emu (Kumar and Singh, 2014).

The present study described the gross morphological features of different bony components of axial, pelvis and the limbs of West African Black-Crowned Crane. Observable features were compared to skeleton of *gruidae* birds and other domestic species described in a conventional avian anatomy textbook. The findings will be useful for comparative anatomy and functional aspects of musculoskeletal system in avian.

## CONFLICT OF INTEREST

The authors have no conflict of interest to declare.

## CONTRIBUTION

Concept and results interpretation-IA; Sample collection and processing-WA, IS; Literature search/Resources-MK, IS; Manuscript writing and critical review-IA, AM.

## REFERENCES

- Choudhary P, Kalita PC, Arya RS, Rajkhowa TK, Doley PJ, Kalita A. 2020. Comparative gross anatomical studies on pelvic limb long bones of crested serpent Eagle (*Spilornis cheela*) and brown wood Owl (*Strix leptogrammica*). *Indian J Anim Res*, 1-6. <http://dx.doi.org/10.18805/ijar.B-3957>.
- Dyce KM, Sock WO, Wensing CSG. 2010. *Veterinary anatomy*. 4th ed. Philadelphia, USA: W.B. Saunders Company.
- Edet DI, Akinyemi AF, Edet AI, Ekwuniah FA. 2018. Conservation the west African BlackCrowned crane (Linn 1758) in the sudano-sahelian wetlands of northern Nigeria. *Int J Avian and Wildlife Biol*, 3(1), 15-9. <http://dx.doi.org/10.15406/ijawb.2018.03.00045>.
- Girgiri IA, Malah MK, Nuhu IS. 2022. Morphology of the sternum, pectoral girdle and wing of west African Black-Crowned Crane (*Balearica pavonina pavonina*) Sahel. *J Vet Sci*, 19(4), 10-5. <http://dx.doi.org/10.54058/saheljvs.v%vi%i.299>.
- Hiraga T, Sakamoto H, Nishikawa S, Muneuchi I, Ueda H, Inoue M, et al. 2014. Vertebral formula in Red-Crowned Crane (*Grus japonensis*) and Hooded Crane (*Grus monacha*). *J Vet Med Sci*, 76(4), 503-50. <http://dx.doi.org/10.1292/jvms.13-0295>.
- Kumar P, Singh G. 2014. Gross anatomy of wing and pelvic limb bones in emu (*Dromaius novaehollandiae*). *Indian J Vet Anat*, 26, 82-6.
- McLelland J. 1990. *A color atlas of avian anatomy*. London, UK: Wolfe Publishing Ltd.
- Moselhy Attia AA, Mohamed SK, El-Ghazali HM. 2018. Anatomical features of bones and bony cavities of the ostrich skull (*Struthio camelus*). *Int J Anat Res*, 6(2-3), 5390-8. <https://doi.org/10.1696/ijar.2018.213>.
- Nickel R, Schummer A, Seiferle E. 1977. *Anatomy of the domestic birds*. 2nd ed. Berlin, Germany: Verlag Paul Parey.
- Olivia P, Christian F. 2020. Birds have pleomorphic skull, too: anatomical network analyses reveal oppositional heterochronies in avian skull evolution. *Commun Biol*, 3, 195. <https://doi.org/10.1038/s42003-020-0914-4>.
- Rezk HM. 2015. Anatomical investigation on the axial skeleton of the cattle egret, *bubulcus ibis*. *Assiut Vet Med J*, 61(145), 12-21. <https://doi.org/10.21608/avmj.2015.169753>.
- Ziermann JM, Diaz Jr RE, Diogo R. 2019. *Heads, Jaws and Muscles: Anatomical, Functional, and Developmental Diversity in Chordate Evolution*. Oxford, UK: Springer Nature.
- Sreeranjini, AR, Ashok N, Indu VR, Lucy KM, Syam KV, Chungath JJ, et al. 2011. Morphological studies on the pelvic girdle of a peahen. *JIVA Kerala*, 9, 46-8.
- Sreeranjini AR, Ashok N, Indu VR, Lucy KM, Maya S, Syam KV. 2013. Morphological studies on the femur, tibiotarsus and fibula of peahen (*Pavo cristatus*). *Tamilnadu J Vet Anim Sci*, 9(4), 248-52.
- Sridevi P, Rajalakshmi K, SivaKumar M. 2020. Comparative gross anatomical studies on femur, tibiotarsus, fibula and tarsometatarsus of great Indian horned owl, flamingo and crow. *J Entomol Zool Studies*, 8(2), 46-55.

## ANATOMIJA AKSIJALNOG I PELVIČNOG SKELETA KOD ZAPADNOAFRIČKOG CRNOKRUNASTOG ŽDRALA (*BALEARICA PAVONINA PAVONINA*)

### SAŽETAK

Istraživanje prikazuje makroskopske morfološke karakteristike kostiju aksijalnog i pelvičnog skeleta odraslog crnokrunastog ždrala. Kostiju su macerirane standardnom tehnikom, pri čemu su prikazani strukturni detalji. Lubanja se sastoji od splahnokranijuma i neurokranijuma, međusobno odvojenim velikom koštanom orbitom. Mandibula predstavlja rostralno dentalnu kost koja sadrži sitne otvore i kaudalno supraangularnu kost. Kranijalni segment vertebralne osovine se sastoji od petnaest cervikalnih i sedam slobodnih torakalnih kralježaka. Kaudalni dio vertebralnog stuba je spojen u jedinstveni koštani stub kojeg čine notarijum i lumbalni sinsakrum, tri srasla primarna sakralna kralješka i tri srasla sinsakrokaudalna kralješka. Postoji šest slobodnih kokcigealnih kralježaka od kojih posljednji predstavlja pigostil. Pelvični pojas je nastao koštanom fuzijom ilijuma, ishijuma i pubisa. Maksimalna dužina femura je iznosila 10,5 cm, a tibiotarzusa 24,5 cm. Tarsometatarzus se sastoji od spojenih II, III i IV metatarzalne kosti koje su uzglobljene sa distalnim nizom tarzalnih kostiju. Crnokrunasti ždral posjeduje četiri funkcionalna prsta. Prvi prst se sastoji od dvije falange, drugi i treći prst od tri i četiri falange, a četvrti prst od pet falangi.

**Ključne riječi:** Aksijalni, crnokrunasti ždral, lubanja, makroskopska anatomija, kosti pelvičnog pojasa